Time Dependence of Nuclear Overhauser Effects of Duplex DNA from Molecular Dynamics Trajectories

Jane M. Withka, S. Swaminathan,† David L. Beveridge, and Philip H. Bolton*

Contribution from the Chemistry Department, Hall-Atwater Laboratories, Wesleyan University, Middletown, Connecticut 06457. *Received November 13, 1990*

Abstract: The buildup rates of nuclear Overhauser effects (NOEs) for all of the protons of a DNA dodecamer have been calculated on the basis of molecular dynamics trajectories of the duplex. The buildup rates were determined by taking into consideration the orientation of the proton-proton vectors to the symmetry axis, the extent of internal motion of the vectors and the interactions between all pairs of protons and the overall anisotropic tumbling of the duplex. The time dependence of the NOEs was determined by solving the generalized Bloch equation by numerical integration for all protons with full relaxation methods. These calculations show that the initial rates of NOE buildups are not always related to the inverse sixth power of the interproton distance. Results also indicate that different simulation models predict distinguishably different experimental data and that, within a particular simulation, distinguishably different experimental data are predicted for distinct residues in the DNA duplex. With these methods, experimental data can be used to discriminate between proposed structural and dynamical models of DNA obtained from molecular dynamics simulations.

Introduction

The determination of the three-dimensional structure of biologically interesting molecules in solution with nuclear magnetic resonance (NMR) and theoretical techniques has become a major area of research over the past several years. Multidimensional NMR techniques have been developed and are capable of obtaining information which can be related to the tertiary structures of proteins and nucleic acids.[1-3] The key questions now are how to interpret NMR data correctly and, subsequently, how to convert this information into the most accurate structural and dynamical models obtainable. Theoretical methods such as molecular dynamics simulation (MD) have become an established approach to the study of structure and dynamics of DNA and other biomolecules.[4-7] However, the accuracy of the resulting structural and dynamical models remains to be verified by experimental data.

In this paper we demonstrate how the structural and dynamical information present in a molecular dynamics simulation can be used to calculate the observable NMR parameters of double helical DNA. The inclusion of anisotropic tumbling of duplex DNA as well as the orientation to the symmetry axis and internal motion of interproton vectors allows calculation of NOE intensities which can be compared directly to experimental data. This approach provides a means for testing the accuracy of the structural and dynamical properties predicted by molecular dynamics on the basis of NMR data. A full description of the molecular dynamics simulation used in the calculation of NMR parameters is given in the accompanying article along with detailed conformational and helicoidal analysis of the generated structures.[7]

The experimental determination of solution structures of nucleic acids and proteins have relied, to a considerable extent, on the experimental distance information present in proton-proton NOEs.[1,2] The optimum approaches for protein and nucleic acid structure determinations may not be the same. For most proteins there are a number of NOEs between residues which are quite distant from one another in sequence and these long-range NOEs can offer significant information about the folding of the protein. For most nucleic acids such as duplex or triplex DNA or RNA (but not ones like tRNA or 5sRNA which have extensive tertiary structure) there are no long-range NOEs comparable to those observed for proteins. Therefore, determinations of nucleic acid structure from NMR data may tend to require more extensive input from theoretical modeling than protein studies. Furthermore, the relatively high density of protons in the backbones of RNA and DNA gives rise to NOE cross-peaks arising from spin diffusion even at the shortest experimentally accessible mixing times, thus complicating the interpretation of NMR data to obtain distances.

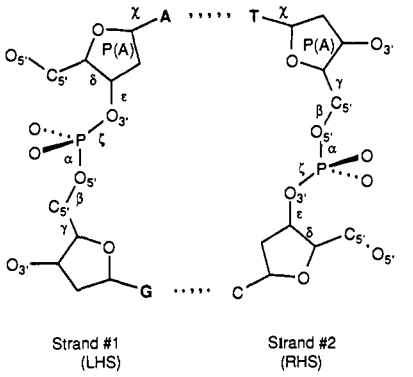

Figure 1. A base pair step and designation of IUPAC conformation parameters[37] used in conformational Dials analysis for nucleic acids.

Estimation of interproton distances from NMR data has been attempted by various approximation methods. The two-spin approximation method[8] is the simplest approach and assumes the initial NOE buildup rate is directly proportional to r_{ij}^{-6}. Since this method does not account for spin diffusion it can lead to inaccurate internuclear distances even in systems containing only three protons.[3] More rigorous treatments, such as those developed by James et al.[9,10] and Kaptein et al.,[11] involve the determination of internuclear distances from iteratively refined molecular models optimized to reproduce the experimental NOE cross-peak intensities. These calculations include all of the proton-proton relaxation interactions but are based on static models of DNA. Since neither the effects of anisotropic tumbling nor the internal

† Bristol-Myers Squibb, Wallingford, CT.

(1) Clore, G. M.; Gronenborn, A. M. *CRC Crit. Rev. Biochem. Mol. Biol.* **1989**, *24*, 479-564.
(2) Wütrich, K. *NMR of Proteins and Nucleic Acids*; Wiley: New York, 1986.
(3) Bolton, P. H. *Prog. NMR Spectrosc.* In press.
(4) Siebel, G. L.; Singh, U. C.; Kollman, P. A. *Proc. Natl. Acad. Sci. U.S.A.* **1985**, *82*, 6537-6540.
(5) van Gunsteren, W. F.; Berendsen, H. J.; Guersten, R. G.; Zwinderman, H. R. *Ann. N.Y. Acad. Sci.* **1986**, *482*, 287-303.
(6) Srinivasan, J.; Withka, J. M.; Beveridge, D. L. *Biophys. J.* **1990**, *58*, 533-547.
(7) Swaminathan, S.; Beveridge, D. L. *J. Am. Chem. Soc.* Preceding paper in this issue.
(8) Spiess, H. W. *Basic Princ. NMR* **1978**, *15*, 54.
(9) Borgias, B. A.; Gochin, M.; Kerwood, D. J.; James, T. L. *Prog. NMR Spectrosc.* **1990**, *22*, 83-100.
(10) Borgias, B. A.; James, T. L. *J. Magn. Reson.* **1990**, *87*, 475-487.
(11) Boelens, R.; Koning, T. M. G.; van der Marel, G. A.; van Bloom, J. H.; Kaptein, R. *J. Magn. Reson.* **1989**, *82*, 290-308.

0002-7863/91/1513-5041$02.50/0

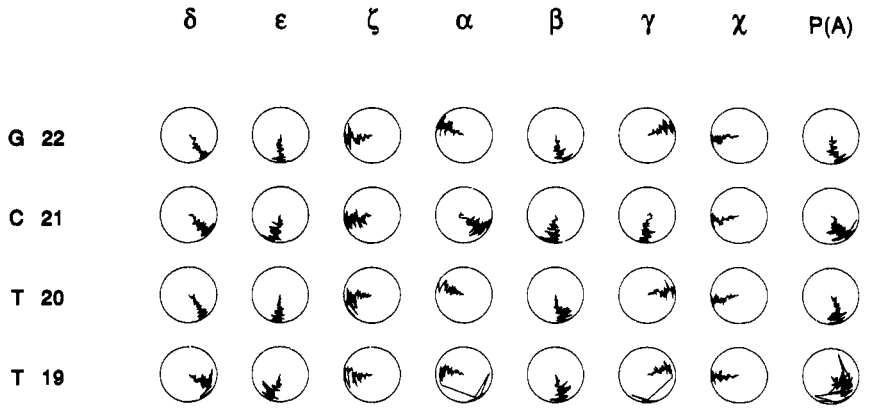

Figure 2. Conformational dials for the analysis of the dynamical behavior of bases T19, T20, C21, and G22. The radial coordinate is the time axis, with t = 60 ps at the center and t = 140 ps at the circumference.

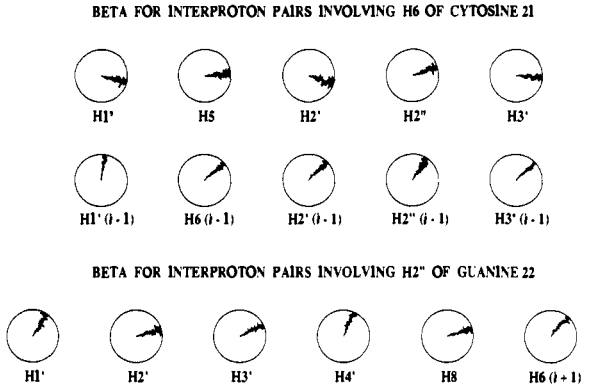

Figure 3. The angle of the internuclear vector, β, to the symmetry axis, z, during the time course of the simulation for proton pairs involving H6 of cytosine 21 (top) and H2″ of guanine 22 (bottom). The radial coordinate is the time axis, with t = 60 ps at the center and t = 140 ps at the circumference.

motion of duplex DNA on the experimental data have been included, inaccurate molecular models may be obtained.

Several approaches to the combined use of NMR data and molecular modeling to investigate DNA have been proposed.[1,2,9-21] One such method has been the use of distance and/or dihedral angle information obtained from interpretation of NMR data as restraints in modeling methods such as molecular dynamics, molecular mechanics, or distance geometry. These restraints have typically been included into the models as potential energy terms with an energy penalty being paid for violation of a distance restraint. Similarly, Case et al.[18] and Sykes et al.[19] have used the intensities of NOE cross-peaks, rather than distances derived from the NMR data, as restraints in the potential energy function.

A different approach is to generate a number of models via molecular dynamics for the DNA duplex under consideration and to use the experimental data to discriminate between the structural and dynamical models. For example, a series of molecular dynamics trajectories could be generated on the basis of judicious modification of the force fields based on the comparison of predicted NOE data with experiment. Each of these trajectories could then be used to calculate the experimental data and the best trajectory selected on the basis of the quality of fit of the predicted results with the experimental data. It is also of interest to have a set of model systems for which the NMR parameters have been calculated, and these models can be used to illustrate which structural and dynamical properties can be reliably detected by NMR.

An attractive feature of this approach is that systematic errors due to a bias in interpreting the experimental data by an overly simplistic method are not introduced. NOEs cannot simply be related to distances in a straightforward manner, and methods following this route can lead to improper structural information as discussed previously and below.[9-11,14-19,21] Additionally, structural perturbations due to the incorporation of inaccurate information or an incomplete set of NOEs in simulations with an added restraint term are eliminated. Furthermore, the use of molecular dynamics without artificial distance or intensity restraints allows approximation of the internal motion of interproton pairs directly from the trajectories. The inclusion of dynamical information in the calculation of NOE intensities allows rigorous comparison of predicted and experimental data.

We have begun to develop a procedure which does not rely on using the experimental data as restraints in at least the first pass at structure determination. In this paper we describe the protocol we are currently using to generate molecular dynamics trajectories and how these trajectories are then used to calculate the NOE buildup curves by full relaxation methods with incorporation of orientation, anisotropic tumbling, and internal motion effects.

The results indicate that different dynamical models predict distinguishably different experimental data, including structural and dynamical features which vary from site to site in the duplex. Therefore, it will be possible to discriminate between models as well as to assess the reliability of the modeling to predict sequence-dependent structural and dynamical variation with use of accessible experimental data.

Generation of Molecular Dynamics Trajectories

Molecular dynamics simulations of the palindromic dodecamer DNA duplex of 5′($C_1G_2C_3G_4A_5A_6T_7T_8C_9G_{10}C_{11}G_{12}$)3′ paired with the self-complementary 5′($C_{13}G_{14}C_{15}G_{16}A_{17}A_{18}T_{19}T_{20}C_{21}G_{22}$-$C_{23}G_{24}$)3′ were performed with WESDYN,[22] a Monte Carlo/molecular dynamics package. The system consisted of the duplex DNA which is fully solvated to provide in excess of two shells of hydration involving 1927 water molecules and 22 Na^+ counterions in a hexagonal prism cell treated under periodic boundary conditions. The potential energy function used in this simulation is

(12) Nerdal, W.; Hare, D. R.; Reid, B. R. *Biochemistry* **1989**, *28*, 10008-10021.
(13) Reid, B. R.; Banks, K.; Flynn, P.; Nerdal, W. *Biochemistry* **1989**, *28*, 10001-10007.
(14) Van de Ven, F. J. M.; Hilbers, C. W. *Eur. J. Biochem.* **1988**, *178*, 1-37.
(15) Clore, G. M.; Gronenborn, A. M. *J. Magn. Reson.* **1989**, *84*, 398-409.
(16) Withka, J. M.; Swaminathan, S.; Bolton, P. H. *J. Magn. Reson.* **1990**, *89*, 386-390.
(17) Withka, J. M.; Swaminathan, S.; Bolton, P. H. *NATO Symp. Ser.* In press.
(18) Yip, P.; Case, D. A. *J. Magn. Reson.* **1989**, *83*, 643-648.
(19) Baleja, J. D.; Pon, R. T.; Sykes, B. D. *Biochemistry* **1990**, *29*, 4828-4839.
(20) Pardi, A.; Hare, D. R.; Wang, C. *Proc. Natl. Acad. Sci. U.S.A.* **1988**, *85*, 8785-8789.
(21) Metzler, W. J.; Wang, C.; Kitchen, D. B.; Levy, R. M.; Pardi, A. *J. Mol. Biol.* **1990**, *214*, 711-736.
(22) Swaminathan, S. *WESDYN*; Wesleyan University: Middletown, CT 1990.

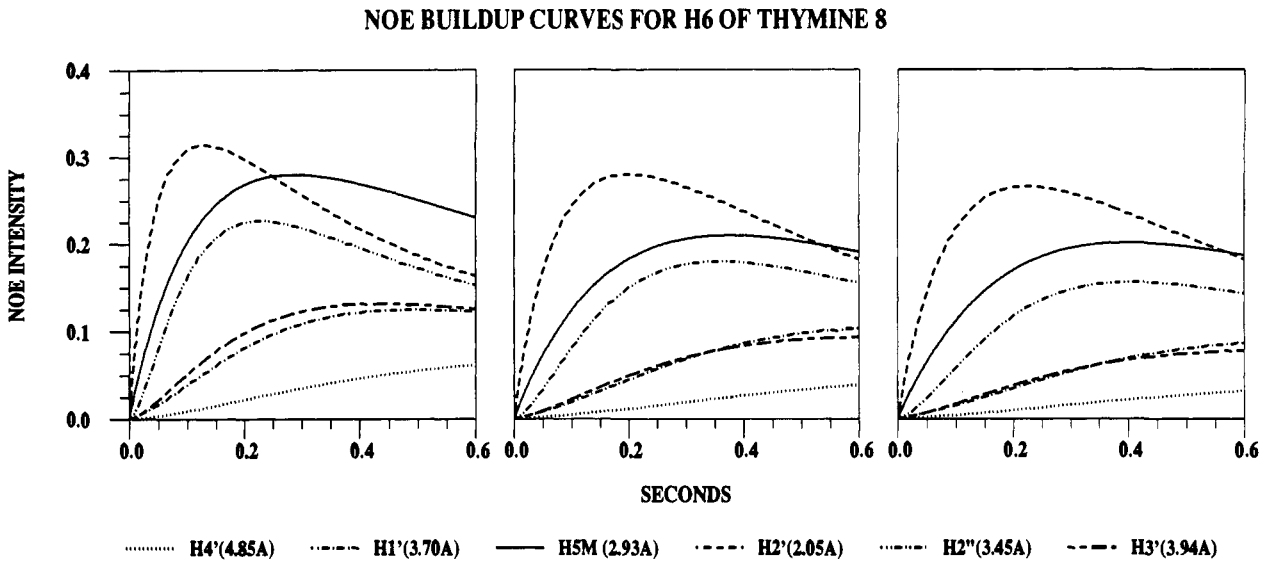

Figure 4. Intraresidue NOE buildup curves for the H6 of thymine 8. The left panel includes buildup curves which depend only on the interproton distance. The middle panel includes effects of orientation and anisotropy of duplex DNA. The right panel includes effects of orientation, internal motion, and anisotropy of duplex DNA. The average interproton distances (Å) are included at the bottom.

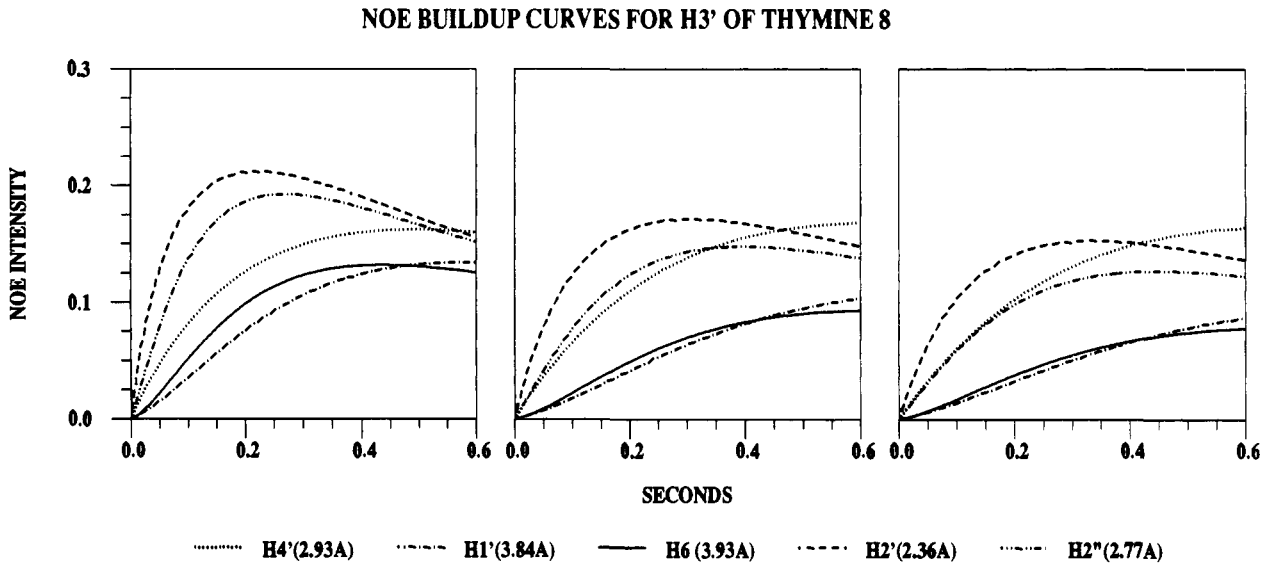

Figure 5. Intraresidue NOE buildup curves for the H3′ of thymine 8. The left panel includes buildup curves which depend only on the interproton distance. The middle panel includes effects of orientation and anisotropy of duplex DNA. The right panel includes effects of orientation, internal motion, and anisotropy of duplex DNA. The average interproton distances (Å) are included at the bottom.

the standard Gromos86 formulation[23] and parameters with the addition of a harmonic constraint function for hydrogen bonds involved in Watson–Crick base pairing. The nonbonded cutoffs for all solute–solute, solvent–solvent, and solute–solvent interactions are 7.5 Å, after which a switching function operates with a cutoff of 8.5 Å. All nonbonded interactions are calculated by group–group interactions in which all assigned chemical subunits are electrically neutral to avoid splitting of dipoles. A dielectric constant of 1.0 is assumed in all electrostatic calculations.

Initial equilibration of the counterion structure was performed by Monte Carlo methods with the solute fixed in the canonical B-DNA form.[24] The solute and counterions were subsequently solvated by the 1927 waters, and simultaneous equilibrations of the solvent and the counterion structure were then carried out by Monte Carlo methods. Upon equilibration of the solvent and counterion environment by stabilization of the total energy, solute-ion energy, and solute–solvent energy, the entire system is energy minimized by conjugate gradient methods for 50 steps and followed by molecular dynamics. The total MD simulation, including heating to 300 °C, equilibration, and trajectory, consisted of 140 ps. These calculations were performed with use of the optimized code on the Cray YMP at the Pittsburgh NSF Supercomputer center. A full description of the calculation and detailed conformational analysis is presented in the accompanying article.[7]

An additional simulation was also examined. This simulation was identical with the one described above with the exception of not having the harmonic constraints for atoms involved in the Watson–Crick base pairs. The constrained simulation is referred to as the "Watson–Crick" (WC) simulation and the unconstrained simulation as the "electrostatic" (ES) simulation. Unless stated otherwise the comments below refer to the WC simulation.

Conformational analysis of the structures generated during the time course of the WC simulation indicates that the structures reside in the B-DNA family with a root-mean-square deviation of ~2.3 Å from the canonical B form, ~2.6 Å from the crystal structure, and ~6.2 Å from the canonical A form. The time

(23) van Gunsteren, W. F.; Berendsen, H. J. C. GROMOS86: Groningen Molecular Simulation System; University of Groningen, The Netherlands 1986.

(24) Arnott, S. personal communication 1980.

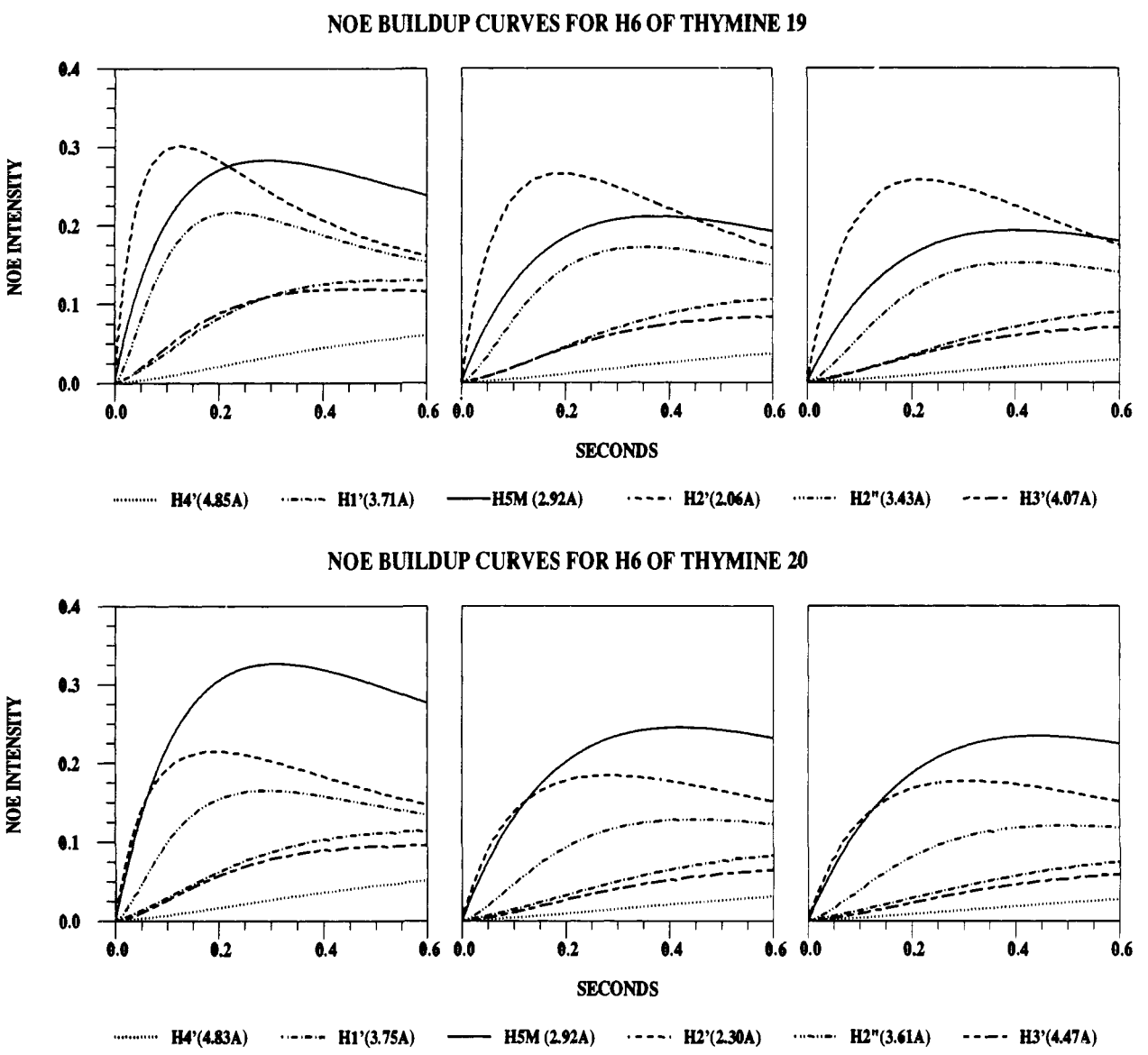

Figure 6. Intraresidue NOE buildup curves for the H6 of thymine 19 (top) and thymine 20 (bottom). In both sets of buildup curves, the left panel includes buildup curves which depend only on the interproton distance. The middle panel includes effects of orientation and anisotropy of duplex DNA. The right panel includes effects of orientation, internal motion, and anisotropy of duplex DNA. The average interproton distances (Å) are included at the bottom.

course of representative phosphodiester torsion angles, as defined in Figure 1, is shown in Figure 2 and can be seen to be relatively stable and to remain close to the canonical B-DNA values. The sugar pucker, described by the pseudorotation angle, P(A), begins at C2′-endo for the canonical B-form and drifts, for some residues, to the C1′-exo state. The exocyclic torsion angles, χ, remain stable and in the B-form range. The torsion angles (α and γ) show correlated changes at some positions in the duplex. These correlated transitions are indicative of a crankshaft motion in which compensatory changes occur while the overall helix remains intact.[7,25]

Overall, the structures generated by molecular dynamics remain in the B-DNA family as indicated by their sugar puckers, backbone torsion angles, and inter-base pair parameter RIS, as well as the position of the bases relative to the axis as determined by XDP. However unlike canonical B-DNA, there is significant angular orientation of the base pairs with respect to the helical axis as indicated by INC.[7] These B-like structures are in qualitative agreement with the solution structure of this dodecamer as determined by two-dimensional NOE data. Helix analysis does indicate bending at C3pG4 and C9pG10 steps which corresponds to primary and secondary hinge points designated to Drew and Dickerson[26,27] in the crystal structure.

To test the ability of our methods to distinguish between simulations on the basis of dynamical and structural information obtained from the trajectory, NOE buildup curves were determined for the ES simulation. During the time course of this simulation bending of the duplex occurred along with disruption of the Watson–Crick hydrogen bonds at base pair 4. It is noted that the disruption of hydrogen bonding at base pair 4 is not accompanied by changes in the backbone torsion angles during the time course of the simulation. However, significant perturbations in the inter-base pair and intra-base pair parameters are detected in the simulation at base pair 4 and smaller disturbances are observed at the neighboring base pairs 5 and 6. The conformational differences in structures from both simulations result in the root-mean-square deviation between the two sets of structures of ~2.0 Å.

(25) Ravishanker, G.; Swaminathan, S.; Beveridge, D. L.; Lavery, R.; Sklenar, H. *J. Biomol. Struct. Dyn.* **1989**, *6*, 669–699.

(26) Dickerson, R. E.; Drew, H. R. *J. Mol. Biol.* **1981**, *149*, 761–786.

(27) Dickerson, R. E. In *Structure and Methods*. Volume 3. *DNA and RNA*; Sarma, R. H., Sarma, M. H., Eds.; Adenine Press: New York, 1990, pp 1–38.

Determination of Time Dependence of NOEs from Molecular Dynamics Trajectories

The approach used here follows from that which we have previously presented and includes all of the non-exchangeable protons.[16,17] It has been widely assumed that the rate of buildup of NOEs can be directly related to the interproton distance through the familiar relationship

$$\sigma_{ij} = \{5.7 \times 10^4/(r_{ij})^6\}\{\tau_e - 6\tau_e/(1 + 4\omega^2\tau_e^2)\}$$

with σ_{ij} the cross-relaxation rate between protons i and j in seconds, r_{ij} the distance between protons i and j in nm, ω the Larmor frequency, and τ_e the effective correlation time. A number of studies have shown that to accurately characterize the relaxation of nucleic acids, which is of primary interest here, consideration of only isolated pairs of spins is not sufficient and all proton–proton interactions need be taken into account as discussed elsewhere.[9,11,14,16,21]

Since double-stranded DNA is an asymmetric molecule and undergoes anisotropic tumbling, the relationship between NOEs and distances is actually a *vector* relationship.[16,17] That is, the NOE buildup rate depends not only on the interproton distance but on the orientation of the proton–proton vector relative to the symmetry axis of the DNA. There are additional effects due to the motion of the internuclear vector relative to the symmetry axis as described below.

A DNA double helix can be modeled to a sufficient level of accuracy as a cylinder with a diameter of 2.05 nm and a length of 0.34 nm per base pair. Thus, a dodecamer will have a length to diameter ratio of about 2. The diffusion rate of a vector along the long symmetry axis will be different than the diffusion rate of a vector along an axis perpendicular to the symmetry axis.[28,29] Consider the case of one proton–proton vector pointing along the symmetry, z, axis and one perpendicular to the z axis along the x axis. Since there will be more rapid motion about the z axis this will cause a proton–proton vector aligned along the x axis to have a shorter effective correlation time than a proton–proton vector aligned along the z axis. Thus the orientation of the interproton vector relative to the symmetry axis as described by the angle β can have a significant effect on NOE buildup rates.

Internal motion in an asymmetric molecule like double-stranded DNA can have pronounced effects on NOE buildup rates due to fluctuations in the local magnetic field with a resultant decrease in the effective correlation time. With use of an approach similar to that recently proposed by Eimer et al.,[30] an expression for the effective correlation time of an internuclear vector can be obtained which is[16,17]

$$\begin{aligned}\tau_e = \{1/4 + 9/(8\exp[4\theta^2]) + (3\cos[2\beta])/(2\exp[2\theta^2]) + \\ (9\cos[4\beta])/(8\exp[4\theta^2])\}/(24D_\perp) + \\ \{3(1 + 1/(2\exp[-4\theta^2]) - (2\cos[2\beta])/\exp[2\theta^2]) + \\ (\exp[-4\theta^2 - 4\zeta^2]\cos[4\beta])/2\}/(16(2D_\perp + 4D_\parallel)) + \\ \{3(\exp[4\theta^2] - \exp[-4\theta^2 - \zeta^2]\cos[4\beta])\}/(8(5D_\perp + D_\parallel)) \quad (1)\end{aligned}$$

with $D_\parallel$ the diffusion constant about the z axis, $D_\perp$ the diffusion constant perpendicular to the z axis, β the angle between the internuclear vector and the z axis, θ the square root of the root-mean-square polar angle of motion, and ζ the square root of the root-mean-square azimuthal angle of motion. When there is no internal motion the above equation reduces to Woessner's equation[29] for the effective correlation time of an asymmetric molecule in which the only motion considered is the diffusion of the cylinder.

The actual value of $D_\parallel/D_\perp$ for a double-stranded DNA such as a dodecamer is not precisely known. Simple hydrodynamics would suggest that $D_\parallel/D_\perp$ goes as $(\text{length})^2/(\text{diameter})^2$. More sophisticated hydrodynamic theories would give corrections to this straightforward expression[30-32] but do not dramatically change the value of $D_\parallel/D_\perp$ from the simple model. The calculations below used $D_\parallel/D_\perp = 3.5$. The value of $D_\perp$ is equivalent to $1/6\tau_\perp$ in which $\tau_\perp$ represents the overall correlation time perpendicular to the symmetry axis which has been determined by depolarized light scattering[30] to be 6 ns for a dodecamer.

Results based on eq 1 have shown that in the presence of internal motion the orientational dependence of the effective correlation time diminishes.[16,17] When the extent of internal motion approaches 25° or so the orientational dependence of the correlation time is somewhat diminished, and when it approaches 45° it is negligible. Thus, as the extent of internal motion increases proton–proton pairs with different β would tend toward having NOE buildup rates which scale simply as a function of the internuclear distance alone. It is also noted that the effective correlation times for all vectors, regardless of β, decrease as the internal motion increases.

The molecular dynamics trajectories performed as described above were used to obtain the average value of β and the value of θ from the fluctuation in β over the course of the trajectory. The dials shown in Figure 3 show the "trajectories" of β for some typical proton–proton vectors. The most significant reductions in the effective correlation time and thus the rates governing relaxation processes are expected for proton pairs with β which approach 90° such as those between the H6–H2′, H6–H5, and H6–H1′ pairs of protons as shown in Figure 3. By using the specific values of β and θ the effective correlation time for each proton pair was obtained and a matrix of inter-proton cross-relaxation rates was constructed for all protons in the DNA dodecamer as described below.

It is noted that the fluctuations in β are typically much smaller, in degrees, than the fluctuation of dihedral bond angles shown in Figure 2. This is due to the fluctuations in β typically being due to motion about several dihedral angles. Therefore, the magnitudes of θ may not be analogous to the motion of single bond vectors, which is the motion detected in ^2H NMR studies of DNA.[33] The extent of internal motion predicted by both the WC and ES simulations, 5–20°, is consistent with the existing body of experimental data.[30]

Calculation of NOE Buildup Rates

The dynamical and distance information utilized in the calculation of the NOE buildup rates was obtained from the last 80 ps of the MD trajectories. Examination of the trajectory indicates that the correlation times of the internal motions of the interproton vectors appear to be less than 50 ps, so the use of 80 ps of trajectory is sufficient to model these motions. The Cartesian coordinate sets were saved and analyzed at 2 ps intervals. All aliphatic and aromatic hydrogens that are not included in the Gromos united atom force field are incorporated into the generated coordinate sets as projections with their Cartesian coordinates determined by the position of the heavy atoms involved. The methyl hydrogens are represented by an average proton which lies in the center of the plane created by the three hydrogens of an idealized methyl group.

The orientation, β, and dynamical information, θ, involved in the direct calculation of the effective correlation times are obtained from the MD trajectory for all proton pairs. The orientation of a proton–proton vector can be described as the angle of this vector with respect to the symmetry axis, z. This angle, denoted as β, is determined for each individual coordinate set throughout the simulation and averaged. The internal motion of a proton–proton vector can be estimated in an MD simulation by calculation of the root-mean-square fluctuation of θ, which represents the angle of each proton–proton vector to its respective average interproton vector. The cross-relaxation and spin–lattice relaxation rates are calculated on the basis of the average interproton vector distance obtained as $\langle r_{ij}^{-3}\rangle^2$ from the MD trajectory with the brackets indicating the time-averaged value.[34]

(28) Lipari, G.; Szabo, A. *J. Am. Chem. Soc.* **1982**, *104*, 4546–4559.
(29) Woessner, D. E. *J. Chem. Phys.* **1962**, *37*, 647–654.
(30) Eimer, W.; Williamson, J. R.; Boxer, S. G.; Pecora, R. *Biochemistry* **1990**, *29*, 799–811.
(31) Tirado, M. M.; Lopez Martinez, M. C.; Garcia de la Torre, J. *Biopolymers* **1984**, *23*, 611–615.
(32) Yoshizaki, T.; Yamakawa, H. *J. Chem. Phys.* **1980**, *72*, 57–69.
(33) Alam, T. M.; Orban, J.; Drobny, G. *Biochemistry* **1990**, *29*, 9610–9617.
(34) Tropp, J. *J. Chem. Phys.* **1980**, *72*, 6035–6043.
(35) Banks, K.; Hare, D. R.; Reid, B. R. *Biochemistry* **1989**, *28*, 6996–7010.

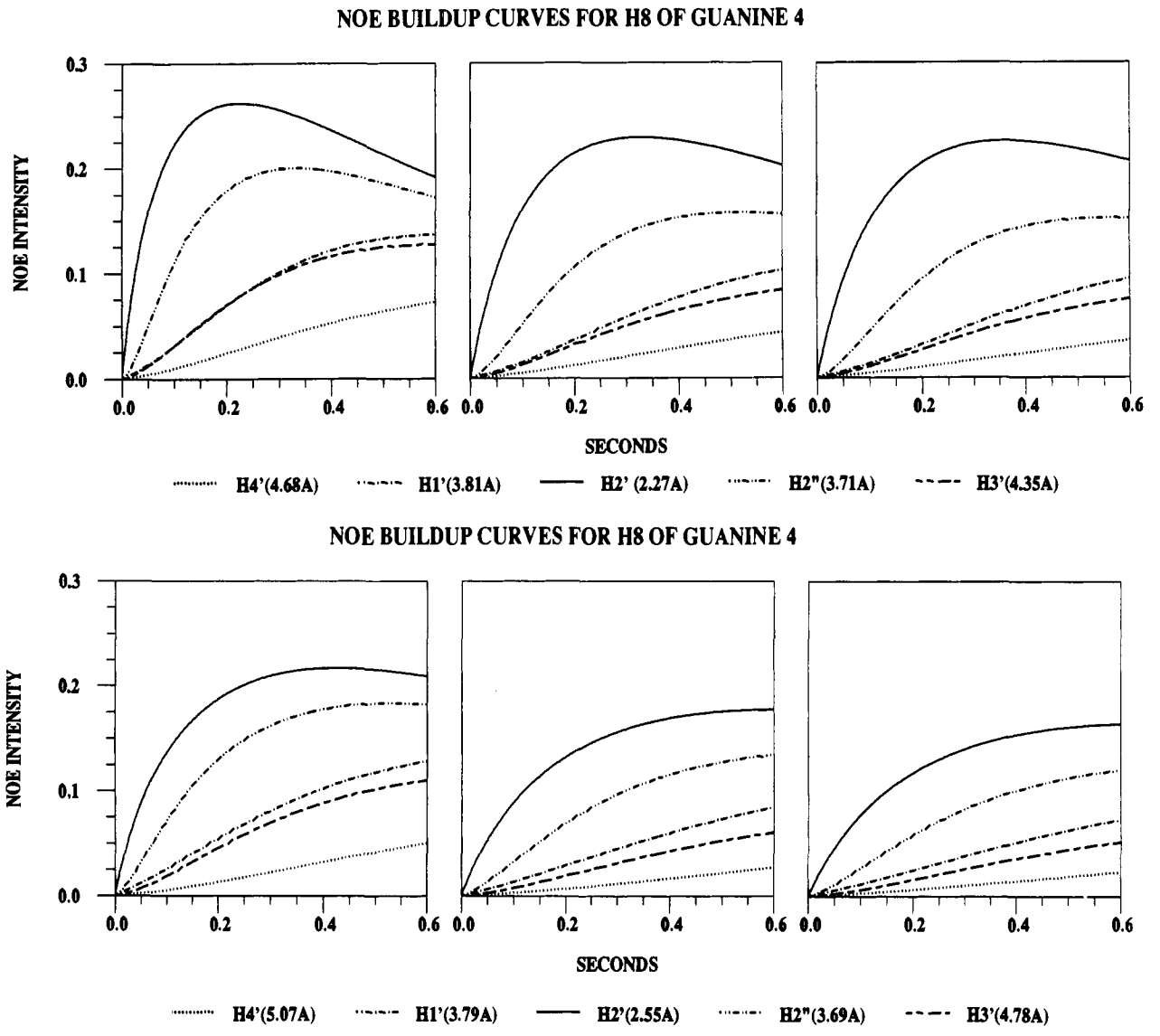

Figure 7. Intraresidue NOE buildup curves for the H8 of guanine 4 in the Watson–Crick (WC) simulation (top) and H8 of guanine 4 in the electrostatic simulation (ES) (bottom). In both sets of curves, the left panel includes buildup curves which depend only on the interproton distance. The middle panel includes effects of orientation and anisotropy of duplex DNA. The right panel includes effects of orientation, internal motion, and anisotropy of duplex DNA. The average interproton distances (Å) are included at the bottom.

As discussed above, the effects of orientation, anisotropic tumbling, and internal motion on the time course of the NOE buildup rates are considered in the calculation of the individual proton–proton correlation times. To present these effects, NOE buildup rates were determined for the three following cases: (i) all proton–proton vectors have a correlation time of 6 ns such that the cross-relaxation σ_{ij} are dependent solely upon the interproton distance; (ii) effective correlation times are dependent upon orientation β and the anisotropy of the duplex; (iii) effective correlation times are dependent upon orientation β and the anisotropy of the duplex as well as the extent of internal motion, θ. For each of the three cases, a matrix of interproton cross-relaxation rates was constructed for all protons in the DNA dodecamer. For protons separated by more than 8 Å the cross-relaxation rate was set to zero since the direct cross-relaxation between such protons is negligible. The cross-relaxation and spin–lattice relaxation rates, ρ_{ij}, can be described in terms of the usual transition probabilities and are shown below:

$$\rho_{ii} = 2(n_i - 1)(W_1^{ii} + W_2^{ii}) + \sum_{j \neq i} n_j(W_0^{ij} + 2W_1^{ij} + W_2^{ij})$$

$$\sigma_{ij} = n_i(W_2^{ij} - W_0^{ij})$$

In this formalism, n_i is equal to the number of equivalent spins in a group and W_0, W_1, and W_2 represent the zero, single, and double transition probabilities, respectively.[8,9] The leakage rate is assumed to be equal to 0.1 and is added to all spin–lattice relaxation rates.

The transition probabilities can be described by

$$W_0^{ij} = \frac{\gamma^4 h^2 \tau_e}{r_{ij}^6} \qquad W_1^{ij} = \frac{3\gamma^4 h^2 \tau_e}{2r_{ij}^6}\left\{\frac{1}{1 + (\omega\tau_e)^2}\right\}$$

$$W_2^{ij} = \frac{6\gamma 4 h^2 \tau_e}{r_{ij}^6}\left\{\frac{1}{1 + 4(\omega\tau_e)^2}\right\}$$

where $\gamma^4 h^2$ is equal to 5.7×10^4 s, ω is the Larmor frequency, r_{ij}^6 is the average interproton distance in nm obtained from the trajectory, and τ_e is the effective correlation time.

The time course of the NOE buildup is then obtained by solving the generalized Bloch equations[8] by numerical integration for all of the 208 protons

$$\frac{dP_i}{dt} = -\rho_{ii}P_i - \sum_{j=1}^{n} \sigma_{ij}P_j n_j \qquad (2)$$

where P_i is equal to the difference in the spin population at time t from the thermal equilibrium value, n_i is equal to the number of equivalent spins in a group, ρ_{ii} is equal to the spin–lattice relaxation rate, and σ_{ij} is equal to the cross-relaxation rate as described above. At time $t = 0$ the initial spin population for the perturbed proton in which the NOE

(36) Nilges, M.; Clore, G. M.; Gronenborn, A. M.; Pie, N.; McLaughlin, L. W. *Biochemistry* **1987**, *26*, 3734–3744.

(37) Davies, D. B.; Altona, C.; Arnott, S.; Danyluk, S. S.; Hruska, F. E.; Klug, A.; Ludeman, H. D.; Pullman, B.; Ramachandran, G. N.; Rich, A.; Saenger, W.; Sarma, R. H.; Sudaralingam, M. *Eur. J. Biochem.* **1983**, *131*, 9–15.

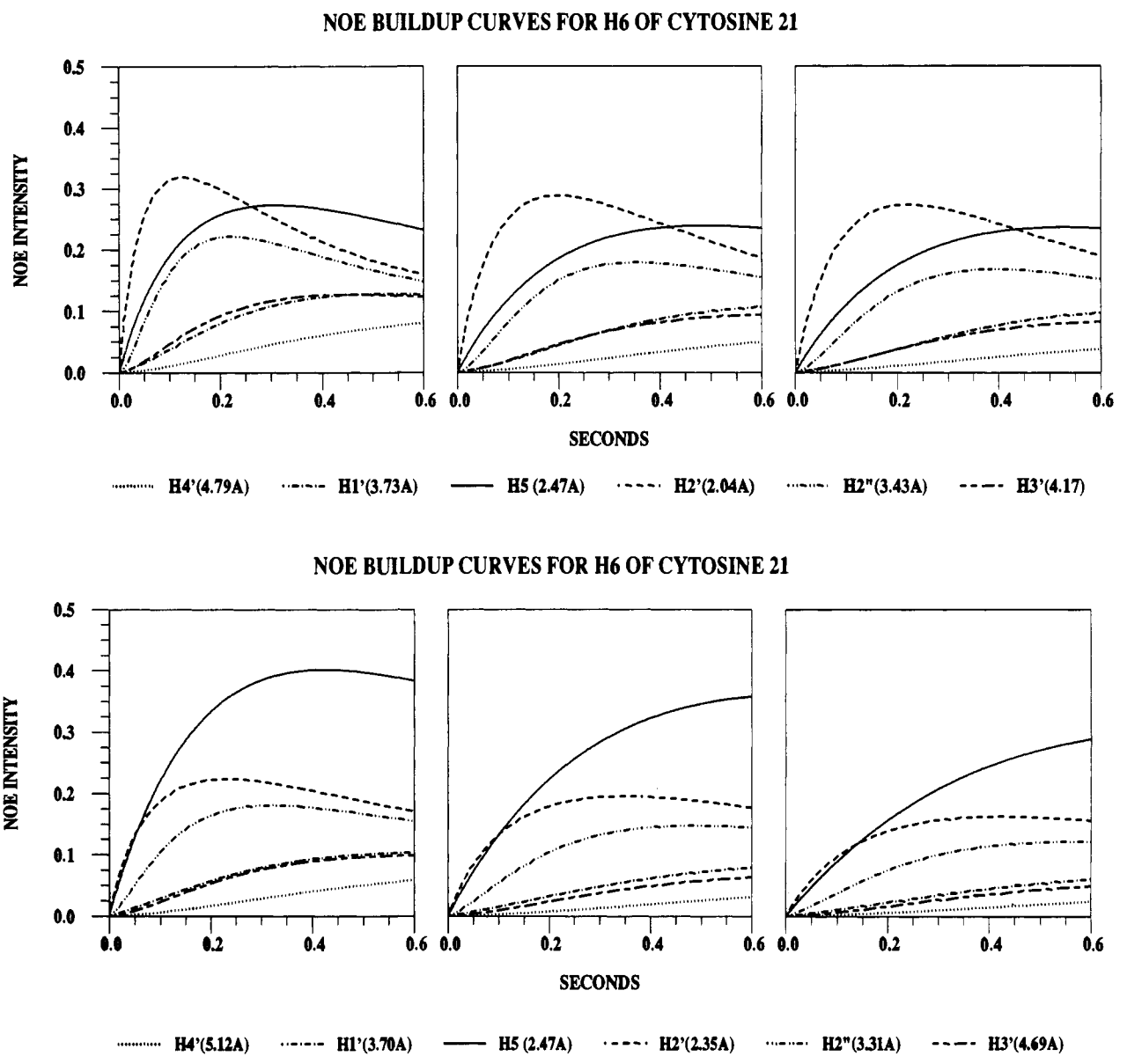

Figure 8. Intraresidue NOE buildup curves for the H6 of cytosine 21 in the Watson-Crick (WC) simulation (top) and H6 of cytosine 21 in the electrostatic simulation (ES) (bottom). In both sets of curves, the left panel includes buildup curves which depend only on the interproton distance. The middle panel includes effects of orientation and anisotropy of duplex DNA. The right panel includes effects of orientation, internal motion, and anisotropy of duplex DNA. The average interproton distances (Å) are included at the bottom.

buildup curves are being generated is set equal to −1.0 while the initial population for all other protons is set equal to +1.0. All thermal equilibrium spin populations are set to +1.0. The change in the spin population is then determined as a function of time, using eq 2, by numerical integration with a time step of 10^{-6} s. Trial runs showed that a time step of 10^{-4} or 10^{-5} s gives results indistinguishable to integrations with smaller time steps. This time coordinate is consistent with the time in which magnetization is allowed to be transferred and is identical with the mixing time in a two-dimensional NOE experiment. In this procedure, both direct and diffusion magnetization transfer occur and both are included in the calculated NOE intensities.[38]

Methyl groups are approximated as an average proton in the central position. This representation of a methyl group as an average proton is incorporated into the calculation of the spin–lattice relaxation and cross-relaxation rates in the following ways: (i) the spin–lattice relaxation rate for the average methyl proton includes a term to represent relaxation among the three methyl protons; (ii) the spin–lattice relaxation rate for any proton which is dipolar coupled to an average methyl proton includes a dipolar contribution which is increased by a factor of 3; (iii) the cross-relaxation rate is increased by a factor of 3 if the average methyl proton is the perturbed proton; and (iv) the magnitude of the cross-relaxation to the average methyl proton from any other proton is increased by a factor of 3.

(38) In the numerical integration approach the entire time course of the NOE buildup curves is calculated whereas in the eigenvalue approach NOE intensities at a particular mixing time are calculated. To determine the NOE buildup curves for a small number of time points the eigenvalue approach is less computationally intensive whereas for the entire buildup curve the numerical integration approach is more appropriate.

Results and Discussion

Typical sets of NOE buildup curves are shown in Figures 4 and 5 to illustrate the magnitudes of including β and θ effects, and the supplementary material contains all of the distance, β, and θ information used in the calculations. In all figures displaying NOE buildup curves, the left panel contains buildup curves which depend only on the interproton distance, the middle panel includes effects of orientation and anisotropy of duplex DNA, and the right panel includes effects of orientation, internal motion, and anisotropy of duplex DNA.

There are several features about the curves that are important.

The first is that the inclusion of the orientation effects can significantly alter both direct and spin-diffusion pathways. For example, this can be observed in Figure 4 for the intraresidue H6-to-H2′, H6-to-H2″, and H6-to-H3′ transfer rates for T8. The rates for H6-to-H2′ transfer are primarily direct at short times while the H6-to-H2″ NOE results from direct transfer as well as indirect transfer from the H2′ proton even at very low mixing times. The H6-to-H3′ transfer occurs primarily via the H2′ and H2″ protons at essentially all mixing times. The inclusion of the orientation effects can change not only the relative magnitudes of the NOE buildup curves but their rank ordering as well.

Second, the curves show that the buildup rate curves are predicted not to be parallel. At short mixing times, this effect is the result of spin diffusion as indicated by a lag phase in the initial phase of the NOE buildup curve. This is apparent in the buildup curves for not only the H6–H3′ case, shown in Figure 4, and the H3′–H6 case, shown in Figure 5, but for many others as well. If the rates depended solely on interproton distances then the ratios of the initial slopes would lead directly to ratios of distances. Thus, some of the buildup curves are not linear with respect to time even at very short mixing times which precludes the direct conversion of some NOE buildup rates into distance information. In the interpretation of NMR data, these effects must be critically evaluated since they are observed in the base-sugar NOEs such as H6/H8–H1′/H3′/H4′ which have been used in determinations of sugar conformation. At longer mixing times, the NOE buildup curves are not parallel due to spin diffusion as well as variations in the rates of other relaxation processes.

The next point is that the inclusion of internal motion, the θ dependence, does not have as pronounced effects as does the inclusion of orientation. The simulations lead to values of θ in the range of 5–20°, and hence while the internal motion effects are smaller than the orientation effects they are still discernable. For example, the rank ordering of the H3′-to-H4′ and H3′-to-H2″ transfer rates shown in Figure 5, is changed when internal motion is included in the calculation of the NOE buildups.

The presentation given above describes how molecular dynamics trajectories were obtained and how these trajectories can be used to predict experimental NMR data. It is important to examine these predictions to determine if the different models predict discernibly different results and if the variation from site to site within a particular model can be distinguished on the basis of experimental data.

The role of sequence dependence in the structure and dynamics of DNA has been investigated with a number of theoretical and experimental approaches. It is clear that in some crystal structures the duplex DNA does exhibit sequence dependence.[26,27] However, in other structures the sequence dependence is much less.[26,27] The role of crystal packing forces on DNA structure is not well understood, and it seems to be the case that DNA duplexes which crystalize in a more regular pattern, such as decamers of B-form DNA, tend to exhibit less site-to-site variation than DNA duplexes which have more irregular crystal forms such as that of the dodecamer discussed here.[26,27] It is noted that while the dodecamer is palindromic and its structure in solution will be symmetric this is not the case in the crystal state presumably due to packing forces.

Some solution-state studies have indicated significant sequence dependence of duplex DNA structure, but it is not clear that the structures determined from the experimental data are reliable since these structures have been determined without regard to the vector nature of the NOEs, and some investigations have also neglected the effects of internal motion and hence incomplete structure determination methods have been used.[12,35,36] Nevertheless, all NMR data to date on the dodecamer have indicated that it is in a conventional B-form structure with all of the residues involved in Watson–Crick base pairing.

The WC simulation leads to a structure for the dodecamer which has a B-form structure, with values for most of the dihedral angles and base pair parameters within the ranges expected for B-DNA.[7] Figures 4–6 show some of the predicted NOEs based on the WC simulation. Of particular interest are the buildup curves for the H6 protons of T20 and T19. The buildup curves are shown in Figure 6 for the cases of neglecting β and θ, including β, and including β and θ. The buildup curves show that the NOE intensities between analogous pairs of protons can vary by as much as a factor of 2. For example, the H6-to-H2′ NOE at a mixing time of about 100 ms is ≈21.4% at residue 19 and ≈12.6% at residue 20 when β and θ are included in the calculation.

Since high-quality experimental data at a mixing time of 100–200 ms, for example, can be used to distinguish between NOEs which vary by a few percent, the variations predicted by this simulation for different sites are well within the range that can be checked against experimental data. A demanding test of the simulation is not only the quality of agreement of the simulation with the data but good agreement with the variation of the predicted NOEs from site to site. Furthermore, all of the NOEs predicted by the simulation should be present in the experimental data and any discrepancy may indicate an error in the model.

The ES trajectory is in most respects analogous to the WC trajectory in terms of the predicted values of β and θ and of dihedral angles and base pair parameters and is discussed in the accompanying article.[7] Of interest is the difference in the predicted NOE buildup curves between the WC and ES simulations especially since the two differ in only the weak harmonic potential for the atoms involved in Watson–Crick base pairing. The comparison of the predicted NOE buildup curves shown in Figures 7 and 8 shows that the differences are well within the range of sensitivity of experimental data. Figure 7 illustrates the contrast in the predicted data for the H8 of G4 and significant differences are seen for the H8–H2′ and H8–H3′ NOE buildup curves. Figure 8 illustrates the contrast in the predicted data for the H6 of C21, and significant differences are seen for the H6–H5 and H6–H2′ NOE buildup curves. These differences between the predicted curves are well within the range that can be discriminated between on the basis of experimental data.

It is noted that the differences between the predictions of the two trajectories as well as the differences predicted for distinct sites from a single trajectory are not maximal at the shortest mixing times but rather for mixing times in the range of about 75 to 200 ms. The rationale for this is that each NOE buildup curve does not depend solely on the distance between two protons. Rather each buildup curve depends not only on the direct NOE transfer pathway but on indirect or spin diffusion pathways as well as the number of alternate routes by which each proton can transfer magnetization.

For example, transfer from H8 to H3′ is via the H2″ and H2′ protons so either increasing the H8 → H2′ and H8 → H2″ transfers or decreasing the rates of the H2″ → H1′ or the H2′ → H1′ transfer, for example, would result in a net increase of the transfer to H3′ without any alteration in the H6-to-H3′ distance. Due to the number of distances, orientations, and internal motions which govern the NOE buildup rates, a typical NOE buildup at 75–200 ms depends on many structural and dynamical factors, and it is the differences in all of these factors which is reflected in the differences between the NOE buildup rates.

In this paper we have presented a procedure by which molecular dynamics trajectories can be used to predict experimental results. The comparison of the predicted with actual results will allow the discrimination between various models used to generate the trajectories. With this method, overall structural differences of approximately 2.0 Å root-mean-square deviation can be clearly distinguished. By examination of local conformational variations it appears this procedure is capable of distinguishing structures which differ by approximately 1.0 Å which is the atomic root-mean-square fluctuation in a trajectory. A detailed comparison of experimental data with that predicted by various trajectories will be presented later as well as the use of other experimental data such as coupling constants.

Acknowledgment. This research was supported, in part, by grants from the American Cancer Society (NP-750) (P.H.B.), the National Institutes of Health (GM-37909) (D.L.B.), and the

Bristol-Myers Squibb Corporation via participation in a State of Connecticut Cooperative High Technology Research and Development Grant (P.H.B. and D.L.B.). J.M.W. is a recipient of a Traineeship in Molecular Biophysics via NIH 1T32 GM-08271 (P.H.B. and D.L.B.). Computer time on the CRAY YMP was provided by the Pittsburgh Supercomputer Center. The assistance of Dr. G. Ravishanker and Mr. F. DiCapua in preparing figures is gratefully appreciated. We thank Ms. J. Srinivasan for providing NMR data for initial analysis.

Supplementary Material Available: Tables of all distance, β, and θ information used in the calculation of NMR parameters (24 pages). Ordering information is given on any current masthead page.

Communications to the Editor

Determination of Interchain NOEs in Symmetrical Dimer Peptides

Miquel Pons* and Ernest Giralt

Department of Organic Chemistry, University of Barcelona Martí i Franquès, 1-11, E-08028 Barcelona, Spain

Received October 10, 1990

A considerable number of peptides and proteins are found in nature as dimers linked by disulfide bridges[1-4] or noncovalent interactions.[5,6] In these cases, there are ambiguities in the assignment of NOE interactions as two protons that show a NOE contact can belong to the same unit or to symmetry-related units. These two interpretations will lead, in general, to completely different conclusions about the structure of the molecule.[7] One particular case occurs when the two protons involved belong, in the intrachain case, to the same spin system, as the NH and CH_α protons in the same residue. In this communication we describe the use of a semiselective TOCSY-NOESY experiment to differentiate between these two types of interaction.

Differentiation between intra- and interchain interactions demands the use of mixed dimers[8] in which the two chains differ, for example, by the substitution of deuterium for one or several of the protons involved, the aim being to *selectively* suppress one of the two types of interaction. Unambiguous results can only be obtained when both NOE-related protons are replaced by deuterium, either in the same (Figure 1b) or in different chains (Figure 1c). The substitution of deuterium for only one proton leads to the same degree of suppression of intra- and interchain NOEs (Figure 1d) and therefore, by itself, cannot differentiate between the two situations.

Deuteration of only one of the protons can still be used unambiguously, provided a through-bond connectivity can be established between the two points prior to the NOESY experiment (Figure 1e). In the TOCSY-NOESY[9] experiment coherence is transferred first through scalar coupling and then through dipolar coupling, and therefore this experiment can be conveniently used to distinguish NOEs between protons with a spin system from those between protons belonging to a symmetry-related, different spin system using single-labeled mixed dimers.

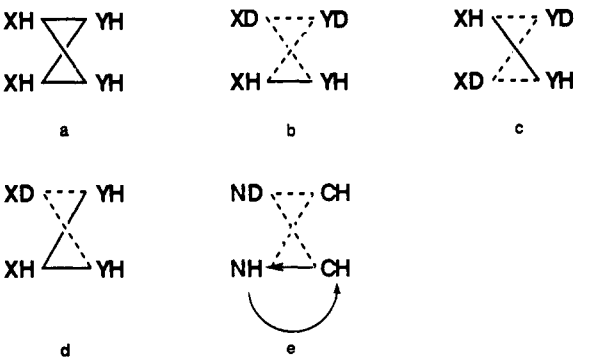

Figure 1. Intra- versus interresidue interactions in a fully protonated sample (a) or in mixed dimers (b-e). Dimers b and c are doubly labeled, and d and e are singly labeled. Full lines represent cross-relaxation pathways leading to the appearance of an NOE, and dashed lines represent suppressed pathways. In e the curved arrow represents magnetization transfer through scalar coupling and therefore implies that the two protons belong to the same spin system. The NOE has also been represented by an arrow to indicate the intrinsic asymmetry of the selective TOCSY-NOESY experiment.

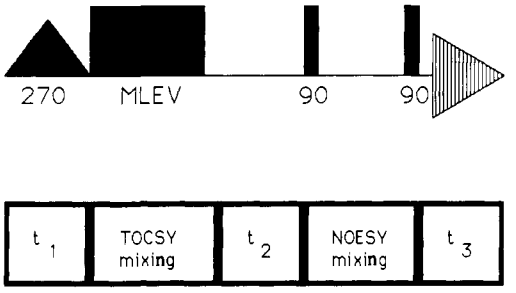

Figure 2. The semiselective TOCSY-NOESY experiment. Semiselective excitation is obtained by a self-refocusing 270° Gaussian pulse.[11] The phases of this pulse and the two 90° hard pulses were cycled as in a conventional NOESY experiment. The phases of the pulses in the MLEV sequence were kept constant. Spectra were recorded in the absolute value mode.

We use a version of the selective TOCSY-NOESY experiment[10] in which the preparation pulse is a 270° Gaussian pulse[11] that excites the complete amide region (Figure 2). A sample of a dimer peptide containing mixed dimers in which only one in each pair of symmetry-related NH protons has been replaced by deuterium can be conveniently obtained by partial exchange with D_2O.

Magnetization derived from the nonexchanged NH protons is spread within the spin system by the MLEV mixing.[12] During the NOESY part of the sequence, magnetization can be trans-

(1) Kangawa, K.; Matsuo, H. *Biochem. Biophys. Res. Commun.* **1984**, *118*, 131-139.
(2) Proux, J. P.; Miller, C. A.; Li, J. P.; Carney, R. L.; Girardie, A.; Delaage, M.; Schooley, D. A. *Biochem. Biophys. Res. Commun.* **1987**, *149*, 180-186.
(3) Tancredi, T.; Temussi, P. A.; Beato, M. *Eur. J. Biochem.* **1982**, *122*, 101-104.
(4) Morize, I.; Surcouf, E.; Vaney, M. C.; Epelboin, Y.; Buehner, M.; Fridlanski, F.; Milgrom, E.; Mornon, J. P. *J. Mol. Biol.* **1987**, *194*, 725-739.
(5) Breg, J. N.; Boelens, R.; George, A. V. E.; Kaptein, R. *Biochemistry* **1989**, *28*, 9826-9833.
(6) Zagorski, M. G.; Bowie, J. U.; Vershon, A. K.; Sauer, R. T.; Patel, D. *Biochemistry* **1989**, *28*, 9813-9825.
(7) Breg, J. N.; Opheusden, J. H. J.; Burgering, M. J. M.; Boelens, R.; Kaptein, R. *Nature* **1990**, *346*, 586-589.
(8) Arrowsmith, C. H.; Pachter, R.; Altman, R. B.; Iyer, S. B.; Jardetzky, O. *Biochemistry* **1990**, *29*, 6332-6341.
(9) Griesinger, C.; Sorensen, O. W.; Ernst, R. R. *J. Magn. Reson.* **1989**, *84*, 14-63.
(10) Sklenář, V.; Feigon, J. *J. Am. Chem. Soc.* **1990**, *112*, 5644-5645.
(11) Emsley, L.; Bodenhausen, G. *J. Magn. Reson.* **1989**, *82*, 211-221.
(12) Levitt, M. H.; Freeman, R. *J. Magn. Reson.* **1981**, *43*, 502-507.

0002-7863/91/1513-5049$02.50/0